Available online at www.sciencedirect.com
ScienceDirect
Ceramics International 37 (2011) 579–583
CERAMICS INTERNATIONAL
www.elsevier.com/locate/ceramint

Fabrication of highly dispersed crystallized nanoparticles of barium strontium titanate in the presence of N,N-dimethylacetamide

Dong Dong, Xiaobo Liu, Haixin Yu, Wencheng Hu *

State Key Laboratory of Electronic Thin Films and Integrated Devices, University of Electronic Science & Technology of China, Chengdu 610054, PR China

Received 15 December 2009; received in revised form 13 January 2010; accepted 26 September 2010
Available online 28 October 2010

Abstract

Highly dispersed nanoparticles of barium strontium titanate (BST) were successfully synthesized by hydrolysis method using N,N-dimethylacetamide as a solvent at 120 °C and 140 °C. X-ray diffraction analysis (XRD) showed that the as-prepared particles presented a perovskite polycrystalline structure. The result of transmission electron microscopy (TEM) images revealed the particle size in the range of 5–30 nm. The composition without any annealing treatment characterized with the parallel plate capacitor method displayed good dielectric properties.

Keywords: C. Dielectric properties; Nanoparticles; Barium strontium titanate; Hydrolysis

1. Introduction

Barium strontium titanate ($Ba_{1-x}Sr_xTiO_3$, BST) material is of considerable interest in electronic industry due to its high dielectric constant and good ferroelectric properties [1]. Barium titanate ($BaTiO_3$) belongs to the perovskite-type structure and is a ferroelectric material with the Curie temperature of 120 °C [2]. $SrTiO_3$ is also the representative ABO_3 type perovskite material, and forms a solid solution with $BaTiO_3$, and the original characteristics of $BaTiO_3$ are still retained. The substitution of Ba by Sr allows the Curie temperature of BST ceramic to decrease linearly [3]. BST powders are widely applied in multi-layer ceramic capacitors [4], microelectronic discrete capacitors [5], capacitance laminates for printed wiring board [6], embedded capacitance materials [7], insulator rings for high power surge arrestors [8], and so on. The dielectric properties of ferroelectric materials depend on the synthesis process, and the purity and morphology of raw materials [9–11]. To achieve fine microstructure and high performance, fine BST powders with stoichiometric composition and narrow size distribution are necessary [12]. The traditional preparation method of BST ceramics, using $BaCO_3$, $SrCO_3$ and TiO_2 as raw materials [13], is a high-temperature solid state reaction, which is not suitable for high performance application because the material has to undergo some defects, such as large particle size, nonhomogeneity and presence of impurities. Various wet chemical non-conventional methods like sol–gel [14], hydrolysis [15], hydrothermal [16], solvothermal [17], combustion synthesis [18], chemical co-precipitation [19] and spray pyrolysis [20] techniques, have been employed to prepare fine BST powders. Sol–gel, hydrolysis and hydrothermal methods, as lower-temperature solution-based synthetic routes, have been confirmed to produce the nanostructure of the ferroelectric products. Among them the hydrolysis of metal alkoxide and acetate is a more attractive method due to its simple synthesis process.

Preparation of ferroelectric powder by hydrolysis method has been widely investigated for different applications. In 1988, Yanovskaya et al. [21] described the simultaneous hydrolysis of lithium and niobium alkoxides followed by heat treatment at 700 °C to prepare the fully crystalline $LiNbO_3$ powder with excellent ferroelectric properties. In 2006, Brutchey et al. [22] readily prepared the nanoparticles of $BaTiO_3$ by kinetically controlled vapor diffusion of $H_2O(g)/HCl(g)$ into the non-aqueous solution of single-source bimetallic alkoxide $BaTi[OCH_2CH(CH_3)OCH_3]_6$ at 16 °C, and the nanoparticles were in situ annealed at 750 °C and 1000 °C causing incremental increase in particle size to 14 and 32 nm. In 2006, Reveron et al. [23] synthesized monocrystalline

* Corresponding author.
E-mail address: huwc@uestc.edu.cn (W. Hu).

0272-8842/$36.00
doi:10.1016/j.ceramint.2010.09.047

nanoparticles of BST with the average particle size ranging from 20 to 40 nm through the hydrolysis method and further crystallization of alkoxide precursors under supercritical conditions. In the present work, barium acetate, strontium acetate and tetrabutyl titanate were employed to prepare highly dispersed crystallized nanoparticles of barium strontium titanate in the presence of N,N-dimethylacetamide.

2. Experimental details

The BST nanoparticles were prepared by the hydrolysis method using barium acetate, strontium acetate and tetrabutyl titanate as the starting materials. N,N-dimethylacetamide and sodium hydroxide were used as a solvent and a pH regulator, respectively. All the reagents above were of analytical purity. In a typical synthesis, 0.026 mol barium acetate and 0.014 mol strontium acetate were dissolved by 50 ml N,N-dimethylacetamide in a 250 ml 3-necked flask, and then the solution with 0.05 mol sodium hydroxide dissolved in 10 ml deionized water was dropped into the mixture while magnetic stirring. Half an hour later, the system was heated to 120 °C or 140 °C in an oil bath, while the atmospheric condenser was essential. 0.04 mol tetrabutyl titanate was gradually dropped into the flask. The mixture was stirred for 2 h at the same temperature, allowing the hydrolysis reaction to take place and forming crystalline nanoparticles of BST. As the sample cooled to room temperature, the BST nanoparticles were obtained by a centrifugal separation at a rotating speed of 10,000 rpm. The samples were washed four times with ethanol to remove the reaction by-products, unreacted starting material and solvent. The washed nanoparticles were dried under vacuum condition at 60 °C for 12 h. For the investigation of dielectric properties of BST nanoparticles, the samples were extruded to form round pieces with a diameter of 10 mm without any binder. As a comparative experiment, N,N-dimethylacetamide was substituted by glycol to repeat the previously described process.

With a rotating target X-ray diffractometer, Ni-filtered Cu Kα radiation was used to determine the composition of the samples by X-ray diffraction (Philips Xpert X-ray diffractometer). A rotating Cu target was employed with a voltage of 40 kV and a current of 100 mA. The morphology was studied using a transmission electron microscopy (TEM; JEM-100CX, JEOL). A 300-mesh copper TEM grid coated with polyvinyl formal was employed with a voltage of 80 kV. Capacitance–voltage, dielectric constant, and loss measurements were carried out using an HP4284A LCR meter.

3. Results and discussion

The previous studies indicated that BST particles prepared at less than 200 °C present the amorphous nature or low degree of crystallinity [24–27], suggesting an incomplete phase formation. The glancing angle X-ray diffraction patterns of the as-prepared BST nanoparticles in the presence of N,N-dimethylacetamide and glycol were shown in Fig. 1. The (1 0 0), (1 1 0), (2 0 0), (2 1 0) and (2 1 1) peaks corresponding to the BST perovskite structure were obtained in the samples synthesized at 120 °C and 140 °C in N,N-dimethylacetamide, and those two samples possessed a non-textured polycrystalline structure with no evidence of secondary phase formation. The X-ray peak intensities showed that the crystallinity of the sample synthesized at 120 °C was evidently worse than the sample synthesized at 140 °C, indicating that the formation of crystalline BST was better at higher temperature. The dimensions of the BST nanoparticles calculated from the widths of the major diffraction peaks exhibited in Fig. 1 (curve a and b) through the Scherrer formula are 11.1 and 12.5 nm. However, from the XRD pattern of the sample prepared in glycol, the peaks were different from the previous two samples. Comparing with the PDF cards, those peaks corresponded to the $Ba_{0.5}Sr_{0.5}CO_3$ (BSC, the number of PDF card is 47-0224) orthorhombic structure and no BST phase existed in this sample. From the intensity, the BSC powders presented an inferior crystallinity, suggesting an incomplete orthorhombic phase formation. Usually, the crystalline $Ba(Sr)CO_3$ nanoparticles can be synthesized at room temperature [28], which means the structure of crystalline $Ba(Sr)CO_3$ is relatively stable at low temperature. From the result, it was obvious that the BST nanoparticles with amorphous structure possess a quite strong chemical activity, and the Ba and Sr ions easily combine with CO_2 existed in air to form orthorhombic BSC nanoparticles. The low CO_2 concentration in air leads to the inferior crystallinity of BSC.

According to earlier investigations [29,30], the crystallinity of particles depends on the dielectric constant of solvent, and nucleation occurs easily in a solvent with a low dielectric constant. The dielectric constants of N,N-dimethylacetamide and glycol are 37.8 and 37.0, respectively at room temperature. However, in alkaline system, N,N-dimethylacetamide should be decomposed to form dimethylamine:

$$CH_3CON(CH_3)_2 + OH^- \rightarrow CH_3COO^- + (CH_3)_2NH$$

Actually, two kinds of solvents co-exist in N,N-dimethylacetamide, although dimethylamine is a volatilizable material. Dimethylamine possesses a low dielectric constant (5.3 at

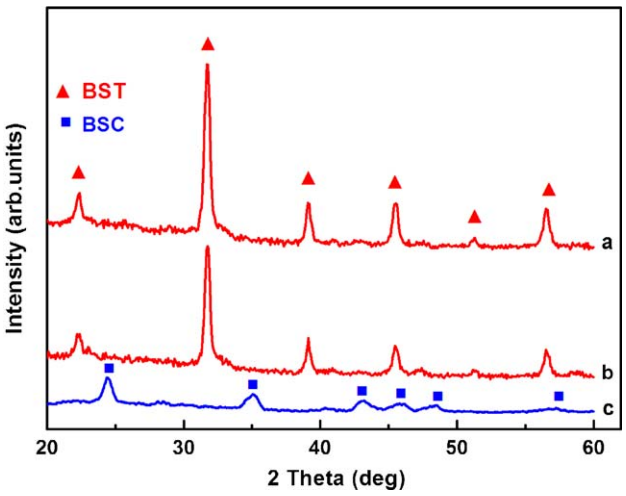

Fig. 1. X-ray diffraction patterns of the nanoparticles prepared in N,N-dimethylacetamide at 140 °C (a) and 120 °C (b), and in glycol at 140 °C (c).

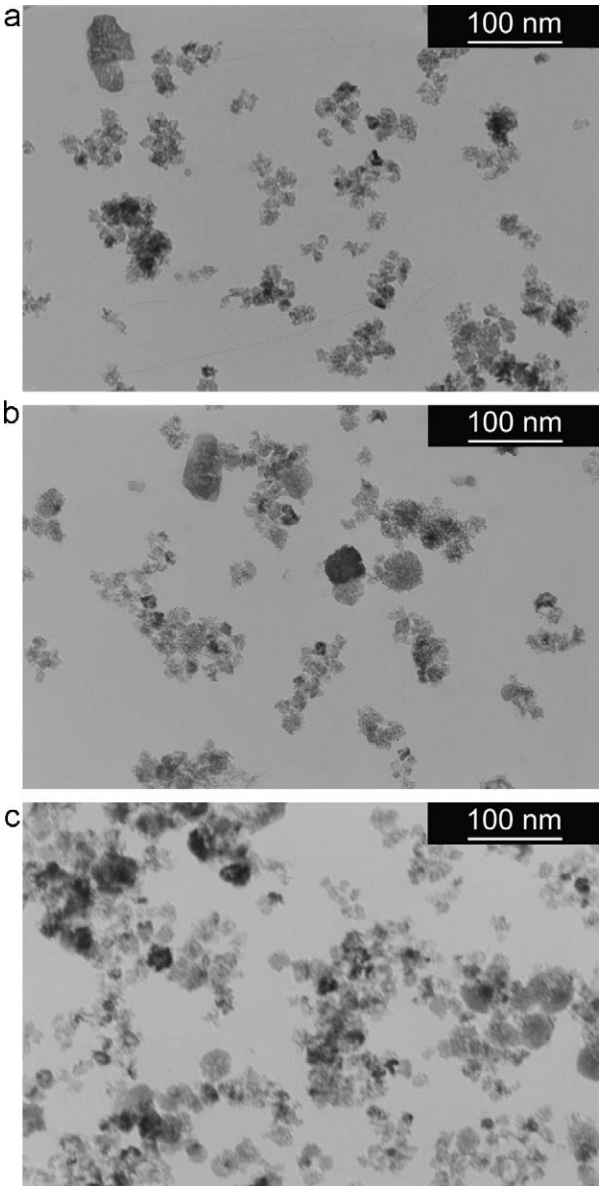

Fig. 2. TEM images of the nanoparticles prepared in N,N-dimethylacetamide at 120 °C (a) and 140 °C (b), and in glycol at 140 °C (c).

2.5 °C) and the dielectric constant of N,N-dimethylacetamide tempestuously decreases with the increase of temperature. Due to the symmetric property of glycol molecules, the increase of temperature has a little influence on its dielectric constant. Such difference is the possible reason leading to the formations of BST crystal in N,N-dimethylacetamide system and BSC crystal in glycol system.

Fig. 2 depicts the typical TEM images of the particles prepared in N,N-dimethylacetamide at 120 °C (a) and 140 °C (b), and in glycol at 140 °C (c). As shown in Fig. 2a and b, fine irregular-shaped particles presented a highly dispersed configuration with different particle size. The particle size was estimated according to TEM to be in the range of 5–30 nm, and the statistical particle sizes are 11 nm and 13 nm, respectively, which is fully consistent with the average particle size deduced from the XRD peaks. Of course, few

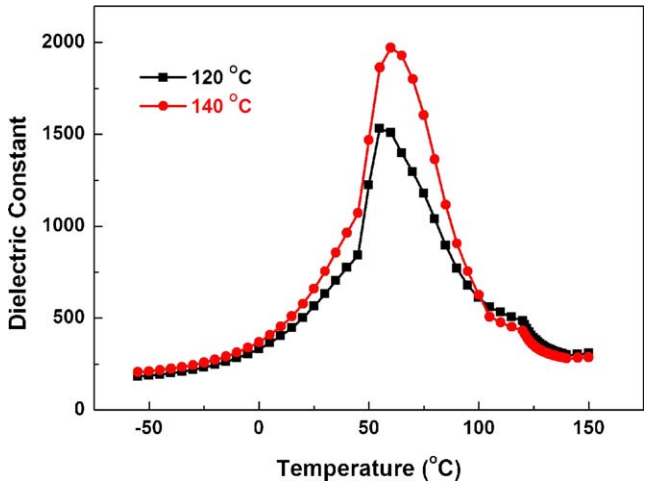

Fig. 3. Dielectric constant as a function of temperature for nanoparticles in the presence of N,N-dimethylacetamide at 120 °C and 140 °C.

agglomerated particles exist in the images, which is a well-known phenomenon in nanoparticle system due to the huge surface Gibbs free energy [31]. However, the agglomerated particles can be easily observed in Fig. 2c. Because the powder synthesized in glycol possesses an inferior crystallinity concluded from XRD results, the particles with an amorphous structure possess higher activity and surface free energy, which leads to more agglomerated particles in glycol system [32].

The dielectric behavior of BST particles synthesized at 120 °C and 140 °C in the presence of N,N-dimethylacetamide without annealing treatment was measured in metal-BST-metal configuration with silver electrodes. The dielectric constant and dielectric loss as a function of temperature was shown in Figs. 3 and 4. The dielectric maximum of those two samples was approximately at around 55–60 °C, corresponding to the transition temperature from ferroelectric phase to paraelectric phase for the composition. The results indicated that the dielectric constant is influenced by the synthesized temperature. It showed a visible increase of dielectric constant as the

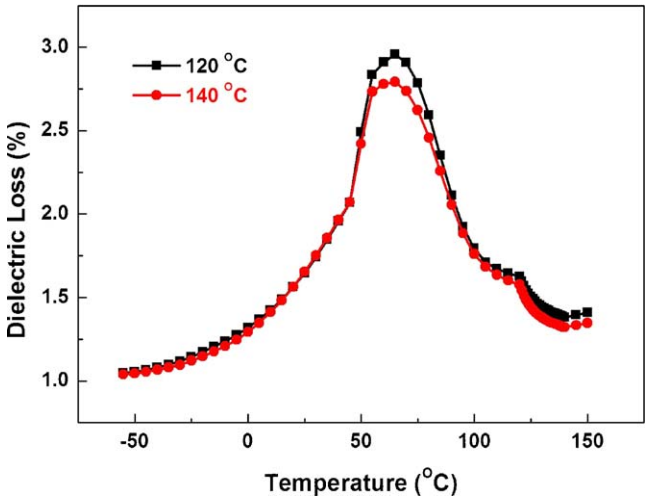

Fig. 4. Dielectric constant as a function of temperature for nanoparticles in the presence of N,N-dimethylacetamide at 120 °C and 140 °C.

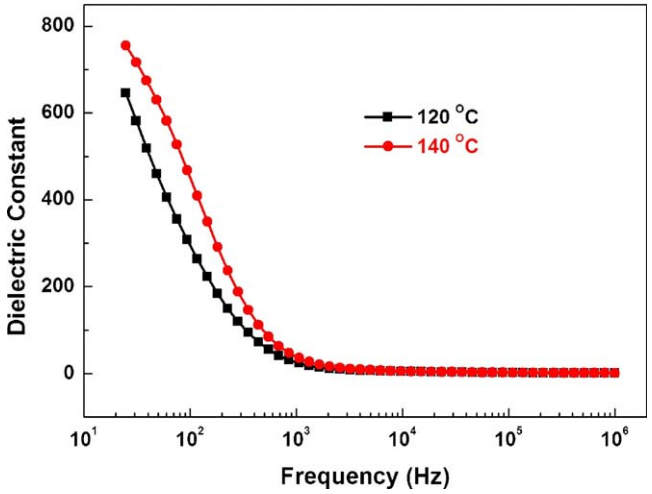

Fig. 5. Dielectric constant as a function of frequency for nanoparticles in the presence of N,N-dimethylacetamide at 120 °C and 140 °C.

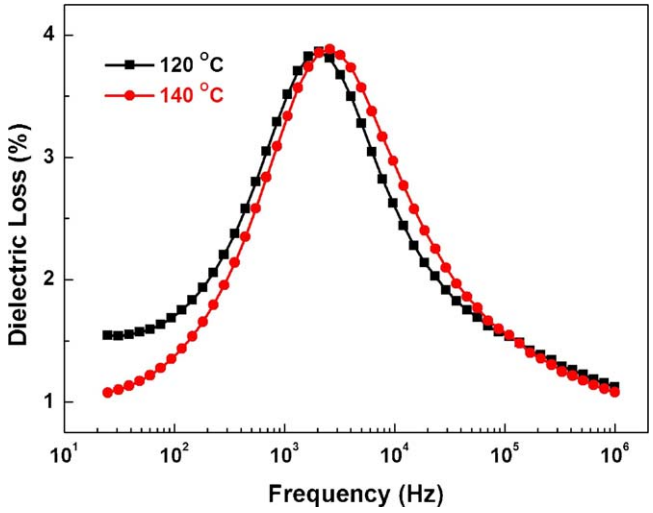

Fig. 6. Dielectric constant as a function of frequency for nanoparticles in the presence of N,N-dimethylacetamide at 120 °C and 140 °C.

synthesized temperature was increased from 120 °C to 140 °C, especially at the point of phase transformation. Fig. 4 shows the dielectric loss data for the samples, and displayed that the loss tangent has no direct relationship with the composition. However, the dielectric loss of the sample synthesized at 140 °C is slightly lower than that of the sample synthesized at 120 °C. It is well known that the dielectric loss includes resistive loss and relaxation loss [33]. The dielectric loss is mainly dominated by mobile charges in the sample, such as oxygen vacancy caused by the non-stoichiometric composition of the samples. The result implies that these defects in the particles are reduced when synthesized at 140 °C.

The dielectric constant and dielectric loss as a function of frequency were measured at room temperature. The result of dielectric constant versus frequency is shown in Figs. 5 and 6. The tendency of the dielectric constant vs. frequency curves is relatively consistent. The abrupt decrease in the dielectric constant with the increase of frequency from 25 Hz to 1 kHz can be easily observed in Fig. 5. Above 1 kHz, the decrease of the dielectric constant values tended towards flattening with the increase of frequency. It has been testified that the size of the individual grain significantly affects the dielectric properties of BST ceramics [34]. The moveable domain walls, which are the intrinsical property of ferroelectric materials, yield a hysteresis that impedes high frequency signals and causes a dielectric relaxation, leading to the reduction of dielectric constant. As the domains are reduced with the decrease of grain size, this relaxation effect has reduced for testable frequencies resulting in frequency stability for nanometer scale grains [35]. From Fig. 6, the tendency of the dielectric loss vs. frequency curves is relatively consistent. As the frequency increased from 25 Hz to 3 kHz, the dielectric loss improved from 1.2% (1.5%) to maximum 3.6% (3.7%). When the frequency further increased, those two curves presented a visible downtrend. This can be ascribed to the reduced relaxation effect under a high frequency leading to the restriction of mobile charges in BST ceramics.

4. Conclusion

We have synthesized ferroelectric nanoparticles of barium strontium titanate by the thermal reaction of barium acetate, strontium acetate and tetrabutyl titanate in N,N-dimethylacetamide. From the result of XRD, the BST nanoparticles presented a polycrystalline structure and the synthesized temperature can affect the crystallinity of the sample. In contrast to the sample prepared in the presence of glycol, the nanoparticles only possessed an inferior crystallinity of $Ba_{0.5}Sr_{0.5}CO_3$ orthorhombic structure. Highly dispersed nanoparticles with the size in the range of 5–30 nm were observed in the typical TEM images. The BST particles were extruded to form round pieces to investigate the dielectric properties. Dielectric-temperature properties indicated that the transition temperatures from ferroelectric phase to paraelectric phase were in the range of 55–60 °C and the dielectric loss varied from 1.1% to 3.7%. In dielectric constant vs. frequency curves, the dielectric constant abruptly decreased to a small value with the increase of frequency. A maximum of dielectric loss was observed in the curves of dielectric loss as a function of frequency. The possible reason was that mobile charges in BST ceramics were restricted by the reduced relaxation effect under a high frequency.

References

[1] S.M. Rhim, S. Hong, H. Bak, O.K. Kim, Effects of B_2O_3 addition on the dielectric and ferroelectric properties of $Ba_{0.7}Sr_{0.3}TiO_3$ ceramics, Journal of the American Ceramic Society 83 (5) (2004) 1145–1148.
[2] W.P. Chen, Z.J. Shen, S.S. Guo, K. Zhu, J.Q. Qi, Y. Wang, H.L.W. Chan, A strong correlation of crystal structure and Curie point of barium titanate ceramics with Ba/Ti ratio of precursor composition, Physica B: Condensed Matter 403 (4) (2008) 660–663.
[3] S. Garcia, R. Font, J. Portelles, R.J. Quinones, J. Heiras, J.M. Siqueiros, Effect of Nb doping on (Sr,Ba)TiO_3 (BST) ceramic samples, Journal of Electroceramics 6 (2) (2001) 101–108.
[4] A. Ries, A.Z. Simoes, M. Cilense, M.A. Zaghete, J.A. Varela, Barium strontium titanate powder obtained by polymeric precursor method, Materials Characterization 50 (2/3) (2003) 217–221.

[5] Y.B. Khollam, S.B. Deshpande, H.S. Potdar, S.V. Bhoraskara, S.R. Sainkar, S.K. Date, Simple oxalate precursor route for the preparation of barium-strontium titanate: $Ba_{1-x}Sr_xTiO_3$ powders, Materials Characterization 54 (1) (2005) 63–74.
[6] Y. Min, A.Z. Phoenix, Method of providing a via opening in a dielectric film of a thin film capacitor, US Patent 0,202,655, 2007.
[7] V. Buscaglia, M. Viviani, M.T. Buscaglia, P. Nanni, L. Mitoseriu, A. Testino, E. Stytsenko, M. Daglish, Z. Zhao, M. Nygren, Nanostructured barium titanate ceramics, Powder Technology 148 (1) (2004) 24–27.
[8] C.D. Dimitrakopoulos, S. Purushothaman, J. Kymissis, A. Callegari, J.M. Shaw, Low-voltage organic transistors on plastic comprising high-dielectric constant gate insulators, Science 283 (5403) (1999) 822–824.
[9] A. Ianculescu, D. Berger, M. Viviani, C.E. Ciomaga, L. Mitoseriu, E. Vasile, N. Dragan, D. Crisan, Investigation of $Ba_{1-x}Sr_xTiO_3$ ceramics prepared from powders synthesized by the modified Pechini route, Journal of the European Ceramic Society 27 (13/15) (2007) 3655–3658.
[10] J.Q. Qia, Y. Wang, W.P. Chen, L.T. Li, H.L.W. Chan, Direct large-scale synthesis of perovskite barium strontium titanate nano-particles from solutions, Journal of Solid State Chemistry 178 (1) (2005) 279–284.
[11] Z. Wang, S.L. Jiang, G.X. Li, M.P. Xi, T. Li, Synthesis and characterization of $Ba_{1-x}Sr_xTiO_3$ nanopowders by citric acid gel method, Ceramics International 33 (6) (2007) 1105–1109.
[12] A. Ianculescua, D. Berger, M. Viviani, C.E. Ciomaga, L. Mitoseriu, E. Vasile, N. Dragan, D. Crişan, Investigation of $Ba_{1-x}Sr_xTiO_3$ ceramics prepared from powders synthesized by the modified Pechini route, Journal of the European Ceramic Society 27 (13/15) (2007) 3655–3658.
[13] J.Y. Wang, X. Yao, L.Y. Zhang, Preparation and dielectric properties of barium strontium titanate glass–ceramics sintered from sol–gel-derived powders, Ceramics International 30 (7) (2004) 1749–1752.
[14] P.K. Sharma, V.V. Varadan, V.K. Varadan, Porous behavior and dielectric properties of barium strontium titanate synthesized by sol–gel method in the presence of triethanolamine, Chemistry of Materials 12 (9) (2000) 2590–2596.
[15] N.J. Ali, S.J. Milne, Comparison of powder synthesis routes for fabricating $(Ba_{0.65}Sr_{0.35})TiO_3$ ceramics, Journal of Materials Research 21 (6) (2006) 1390–1398.
[16] S.B. Deshpande, Y.B. Khollam, S.V. Bhoraskar, S.K. Date, S.R. Sainkar, H.S. Potdar, Synthesis and characterization of microwave-hydrothermally derived $Ba_{1-x}Sr_xTiO_3$ powders, Materials Letters 59 (2/3) (2005) 293–296.
[17] Y.V. Kolen'ko, K.A. Kovnir, I.S. Neira, T. Taniguchi, T. Ishigaki, T. Watanabe, N. Sakamoto, M. Yoshimura, A. Novel, Controlled, and high-yield solvothermal drying route to nanosized barium titanate powders, Journal Physical Chemistry C 111 (20) (2007) 7306–7318.
[18] K.S. Martirosyan, M. Iliev, D. Luss, Carbon combustion synthesis of nanostructured perovskites, International Journal of Self-Propagating High-Temperature Synthesis 16 (1) (2007) 36–45.
[19] Y.B. Khollam, S.V. Bhoraskar, S.B. Deshpande, H.S. Potdar, N.R. Pavaskar, S.R. Sainkar, S.K. Date, Simple chemical route for the quantitative precipitation of barium–strontium titanyl oxalate precursor leading to $Ba_{1-x}Sr_xTiO_3$ powders, Materials Letters 57 (13/14) (2003) 1871–1879.
[20] G. Brankovic, Z. Brankovic, M.S. Goes, C.O. Paiva-Santos, M. Cilense, J.A. Varela, E. Longo, Barium strontium titanate powders prepared by spray pyrolysis, Materials Science and Engineering B 122 (2) (2005) 140–144.
[21] M.I. Yanovskaya, E.P. Turevskaya, A.P. Leonov, S.A. Ivanov, N.V. Kolganova, S.Y. Stefanovich, N.Y. Turova, Y.N. Venevtsev, Formation of $LiNbO_3$ powders and thin films by hydrolysis of metal alkoxides, Journal of Materials Science 23 (2) (1988) 395–399.
[22] R.L. Brutchey, D.E. Morse, Template-free, low-temperature synthesis of crystalline barium titanate nanoparticles under bio-inspired conditions, Angewandte Chemie International Edition 45 (39) (2006) 6564–6566.
[23] H. Reveron, C. Elissalde, C. Aymonier, C. Bousquet, M. Maglione, F. Cansell, Continuous supercritical synthesis and dielectric behaviour of the whole BST solid solution, Nanotechnology 17 (14) (2006) 3527–3532.
[24] Y.B. Khollam, S.B. Deshpande, H.S. Potdar, S.V. Bhoraskar, S.R. Sainkar, S.K. Date, Simple oxalate precursor route for the preparation of barium–strontium titanate: $Ba_{1-x}Sr_xTiO_3$ powders, Materials Characterization 54 (1) (2005) 63–74.
[25] J.L. Zhao, X.H. Wang, R.Z. Chen, L.T. Li, Synthesis of thin films of barium titanate and barium strontium titanate nanotubes on titanium substrates, Materials Letters 59 (18) (2005) 2329–2332.
[26] R.A. Padam, J. Pika, K.G. Ashok, Synthesis, characterization and dielectric properties of nanometer-sized barium strontium titanates prepared by the polymeric citrate precursor method, Journal of Materials Chemistry 13 (2) (2003) 415–423.
[27] K.A. Razak, A. Asadov, J. Yoo, E. Haemmerle, W. Gao, Structural and dielectric properties of barium strontium titanate produced by high temperature hydrothermal method, Journal of Alloys and Compounds 449 (1/2) (2008) 19–23.
[28] L. Chen, Y.H. Shen, A.J. Xie, J.M. Zhu, Z.F. Wu, L.B. Yang, Nanosized barium carbonate particles stabilized by cetyltrimethylammonium bromide at the water/hexamethylene interface, Crystal Research and Technology 42 (9) (2007) 886–889.
[29] X.B. Zhao, X.H. Ji, Y.H. Zhang, B.H. Lu, Effect of solvent on the microstructures of nanostructured Bi_2Te_3 prepared by solvothermal synthesis, Journal of Alloys and Compounds 368 (1/2) (2004) 349–352.
[30] Q.Q. Wang, G. Xu, G.R. Han, Solvothermal synthesis and characterization of uniform CdS nanowires in high yield, Journal of Solid State Chemistry 178 (9) (2005) 2680–2685.
[31] M. Shen, Y. Sun, Y. Han, R. Yao, C.G. Yan, Strong deaggregating effect of a novel polyamino resorcinarene surfactant on gold nanoaggregates under microwave irradiation, Langmuir 24 (22) (2008) 13161–13167.
[32] D. Ozkaya, Particle size analysis of supported platinum catalysts by TEM, Platinum Metals Review 52 (1) (2008) 61–62.
[33] M.S. Tsai, S.C. Sun, T.Y. Tseng, Effect of oxygen to argon ratio on properties of $(Ba,Sr)TiO_3$ thin films prepared by radio-frequency magnetron sputtering, Journal of Applied Physics 82 (7) (1997) 3482–3487.
[34] S. Tusseau-Nenez, J.P. Ganne, M. Maglione, A. Morell, J.C. Niepce, M. Pate, BST ceramics: effect of attrition milling on dielectric properties, Journal of the European Ceramic Society 24 (10-11) (2004) 3003–3011.
[35] M.P. McNeal, S. Jang, R.E. Newnham, The effect of grain and particle size on the microwave properties of barium titanate, Journal of Applied Physics 83 (6) (1998) 3288–3297.